IET Renewable Power Generation

Research Article

IET Journals
The Institution of Engineering and Technology

PVHybNet: a hybrid framework for predicting photovoltaic power generation using both weather forecast and observation data

ISSN 1752-1416
Received on 28th November 2018
Revised 5th November 2019
Accepted on 19th December 2019
doi: 10.1049/iet-rpg.2018.6174
www.ietdl.org

Berny Carrera[1], Min-Kyu Sim[2] ✉, Jae-Yoon Jung[1]

[1]*Department of Industrial and Management Systems Engineering, Kyung Hee University, 1732, Deogyeong-daero, Giheung-gu, Yongin-si, Gyeonggi-do 17104, Republic of Korea*

[2]*Department of Industrial and Systems Engineering, Seoul National University of Science and Technology, 232 Gongneung-ro, Nowon-gu, Seoul 01811, Republic of Korea*

✉ *E-mail: mksim@khu.ac.kr*

Abstract: Photovoltaics has gained popularity as a renewable energy source in recent decades. The main challenge for this energy source is the instability in the amount of generated energy owing to its strong dependency on the weather. Therefore, prediction of solar power generation is important for reliable and efficient operation. Popular data sources for predictors are largely divided into recent weather records and numerical weather predictions. This study proposes adequate deep neural networks that can utilise each data source or both. Focusing on a 24-hour-ahead prediction problem, the authors first design two deep neural networks for prediction: a deep feedforward network that uses the weather forecast data and a recurrent neural network that uses recent weather observations. Finally, a hybrid network, named PVHybNet, combines the both networks to enhance their prediction performance. In predicting the solar power generation by Yeongam power plant in South Korea, the final model yields an R-squared value of 92.7%. The results support the effectiveness of the combined network that utilises both weather forecasts and recent weather observations. The authors also demonstrate that the hybrid model outperforms several machine learning models.

1 Introduction

1.1 Motivation

Sunlight delivers heat and light to all living creatures on earth. Solar power is the conversion of solar energy into electricity using photovoltaic (PV) systems. Solar energy has become popular as a pollution-free energy source; it alleviates the pollution problem by replacing fossil fuels such as crude oil, natural gas, and coal. Unlike fossil fuels, the amount of raw materials for PV generation cannot be controlled by humans. Since smart grid operators aim to manage the supply and demand of energy efficiently and reliably, it is desirable to predict PV generations in advance.

Prediction of PV generation is a multivariate problem, which involves external climate factors and internal factors associated with the power plant facility. For example, a high angular position of the sun, high ambient temperatures, clear skies, low atmospheric humidity, and well-equipped power plants are all likely to increase the energy generation. This study focuses on the prediction problem of the energy generation level using climate factors around the power plant.

Of the many possible approaches discussed in the literature review of the next subsection, we elect to build deep neural networks that generate prediction models utilising large data without being explicitly programmed. The deep neural network technique is known to be effective in approximating multivariate data. This study proposes deep neural networks that can utilise relevant data sources including solar elevation, weather forecast, and weather observations.

1.2 Literature review

With the advent of PV systems, several prediction methods have been studied. Popular predictors include past records of production levels of PV systems and past/current weather information.

In utilising weather information as predictor, a choice is usually made between using weather forecast data or historical weather data. Weather forecast data have been more popular choice [1–9], because weather forecast corresponding to future operation times are generally available. Nonetheless, we note the importance of the rich informational content of recent weather observation for the three reasons. First, weather conditions contain temporal dependencies that can contribute to solar power prediction [10–15]. Second, weather observations by weather agencies tend to contain more variables than weather forecasts. Lastly, weather records are accurate, and they are reported in finer unit. This suggests that some weather-related information may be missing if only weather forecast variables are utilised. For this reason, a few studies select a few variables from weather observations along with the weather forecast data [16, 17]. Though both weather forecasts and recent weather observation records are informative in future PV power generation, there is little study that uses both data sources. Thus, this study builds a model that utilises an extensive number of weather-related variables including both weather forecasts and past weather observations.

In addition to the source of predictors, prediction methods are another important criterion for classifying existing studies. Popular prediction methods can be largely divided into three categories: physical methods, statistical methods, and hybrid methods [18–20].

Physical methods attempt to predict solar altitude and the resulting solar radiation without using other climate data [21, 22]. While this approach may be effective for predicting the single most important variable, solar radiation, it requires a separate model for each specific location of each PV plant. In addition, this approach is likely to overlook relevant information contained in weather fluctuations.

Statistical methods can be further classified into two types of methods: classical regressive methods and statistical learning-based methods [18]. Regressive methods entail regression analysis that may adopt a time-series form. A representative example of non-time-series regression model is Kim *et al.* [15] who use both historical operating data and weather forecast data. More existing studies adopt time-series regression. Bacher *et al.* [11] adopt an auto-regressive model with weather observation. Li *et al.* [4] adopt an auto-regressive moving average model in which weather forecast data of solar irradiance are used as the input. A few studies have been devoted to compare the performances of statistical

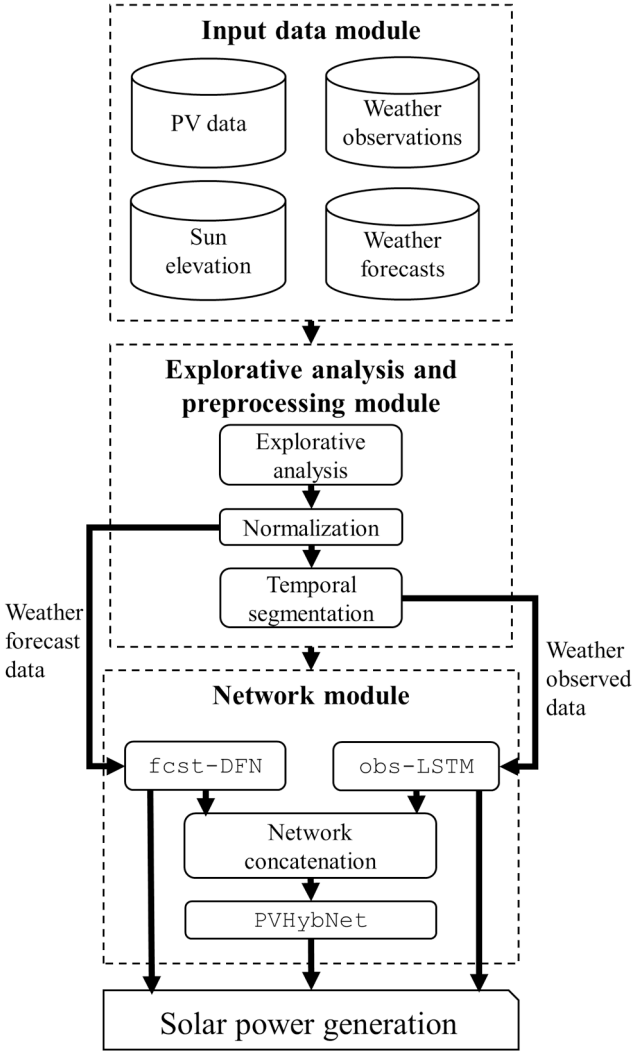

Fig. 1 *Framework of the proposed method*

learning-based methods such as linear regression, bagging, decision trees, random forests, support vector machines, and generalised additive models [12, 19, 23]. These studies commonly find random forests as the best performing algorithm. More recent studies implement gradient boosting regression trees using weather forecast data [5, 9]. This study compares the performance of the proposed deep neural network-based model against that of several widely used machine learning methods.

Lastly, hybrid methods utilise a combination of not only statistical approaches but also different types of techniques such as mathematical optimisation, signal processing, or feature selection. Abedinia *et al.* [17] preprocess historical solar power and weather forecast data using normalisation and signal processing techniques. Their forecasting engine uses learning algorithms based on mathematical optimisation and deep feedforward networks (DFNs). Abuella and Chowdhury [24] combine individual forecasting models to perform predictions. Interestingly, they incorporate the ramp rate of the solar power generation into their ensemble learning approach.

Since this study adopts deep neural networks, we shall further investigate existing prediction studies based on deep neural networks. Two branches of algorithms are most popular: DFNs and recurrent neural networks (RNNs). Pedro and Coimbra implement a DFN and exhibit that the generated model outperforms other approaches including k-nearest neighbours and auto-regressive integrated moving average (ARIMA) [25]. DFN is a widely used choice for 24-hour-long prediction using weather forecast data in other studies as well [6, 7]. Among the family of RNNs, the long short-term memory (LSTM) networks are well known to provide better performance than the vanilla RNN [26], and widely used for other applications as well [27–30]. Thus, several studies implement LSTM networks to capture the temporal dependence of the predictor variables [8, 13, 14, 26]. These studies used following predictors: weather forecast data [8], weather observations data [13, 14], and only PV data itself (univariate model) [31].

Since weather forecast is targeted for a future time and the timestamp can be matched to the future PV generation, DFN can be used to process weather forecast. On the other hand, under the hypothesis that past weather records contain temporal dependencies, a time-series version of deep neural network, RNN, is more suitable. Thus, this study proposes three networks that are a DFN for weather forecast (fcst-DFN), a LSTM for weather observations (obs-LSTM), and a hybrid network for both (PVHybNet). In our knowledge, no previous study has attempted to combine two types of deep neural networks to achieve the benefit of the both.

This study implements both DFN and RNN, aiming to achieve benefits of the both networks. Specifically, we first implement a DFN whose input is weather forecasts, named fcst-DFN, and a LSTM network whose input is weather observations, named obs-LSTM. The final network, named PVHybNet, then combines the two networks to seek their benefits. The combination of these cutting-edge neural networks expands and generalises most previous studies that use statistical approaches. Although this study only adopts statistical approaches, the final network PVHybNet can be considered a hybrid approach since two different types of neural networks are combined.

1.3 Paper organisation

The rest of this paper is organised as follows. Section 2 presents a brief overview of the proposed framework. Section 3 describes the input dataset, explorative data analysis, and preprocessing. Section 4 develops the predictive methods: DFN, LSTM network, and the network combining the DFN and the LSTM network. Section 5 presents the key results along with a comparison against previously reported models. Section 6 concludes the paper.

2 Framework for predicting solar power generation

The framework consists of three modules as depicted in Fig. 1. The input data module collects the PV data from the Korea Open Data Portal (KODP) [32], the solar elevation data from Stellarium® [33], and weather-related data from the Korea Meteorological Administration (KMA) [34]. For PV data, the historical power generation data of Yeongam solar power plant located in Yeongam, Jeollanam-do, South Korea is collected from KOPD. Solar elevation is the vertical angular position of the sun relative to the horizon. The data are collected from Stellarium, an open source planetarium software that provides the spatial positioning of many stars including the sun. The KMA provides weather observation data and weather forecast data. The weather data of this study are collected at the nearest weather station from the solar power plant.

The explorative analysis and preprocessing module contains three steps: explorative analysis, normalisation, and temporal segmentation. The explorative analysis briefly explores how each variable relates to the level of power generation. Then, a few variables are removed for prediction if (i) the variable is obviously unrelated or (ii) the variable is highly correlated with another candidate predictor and its importance is clearly less than the others. The normalisation step converts the data into a bounded interval so that they can be fed to deep neural networks. Since LSTM network takes the input data in the form of time-series vectors, the temporal segmentation step preprocesses the weather observation data into LSTM feed format.

The network module constructs the three deep neural networks. First, the fcst-DFN network is created to use the weather forecast as the primary predictors and to process inputs by DFN. Second, the obs-LSTM network is created to use the weather observation as the primary predictors and to process inputs by LSTM network. Finally, the PVHybNet network is created by concatenating the outputs of the two previous networks.

Table 1 Dependent and independent variables

Variable	Description (unit)
(a) Solar power generation	
generation	solar power generation (kWh)

Variable	Description (range)
(b) Solar elevation	
elevation	solar elevation (0°–76°)

Variable	Description (unit)
(c) Weather forecast	
humidity	(%)
RainfallProbability	(%)
RainfallType	0: none, 1: rain, 2: sleet, 3: snow
SkyType	1: clear sky, 2: slightly cloudy, 3: partly cloudy, 4: overcast
Temperature	(°C)
WindDirection	east: 45°–135°, south: 135°–225°, west: 225°–315°, north: 315°–45°
WindSpeed	(m/s)

Variable	Description (unit)
(d) Weather observation	
AirTemperature	(°C)
AtmospherePressure	(hPa)
DewPointTemperature	temperature at which the air cannot hold all the water vapour (°C)
GroundTemperature	(°C)
humidity	(%)
precipitation	(mm)
SeaLevelPressure	(hPa)
SolarRadiation	(MJ/m^2)
SunlightTime	(h)
VaporPressure	(hPa)
WindDirection	east: 45°–135°, south: 135°–225°, west: 225°–315°, north: 315°–45°
WindSpeed	(m/s)
5 cm-GroundTemperature	temperature below the earth's surface (°C)
10 cm-GroundTemperature	
20 cm-GroundTemperature	
30 cm-GroundTemperature	

Variable	Description (unit)
(e) Temporal variables	
Weeknum	week index (1–53)
TimeIndex	1: 5 am–8 am, 2: 8 am–11 am, 3: 11 am–2 pm, 4: 2 pm–5 pm, 5: 5 pm–8 pm

3 Explorative analysis and preprocessing

This section describes the dataset used in this study. The data collection period is spanned for three years, from January 2013 to December 2015. Table 1 lists the variables. The dependent variable of solar power generation is described in Section 3.1. The independent variables such as solar elevation, weather forecast, and weather observation are described in Sections 3.2–3.4, respectively. Additionally, temporal variables such as Weeknum and TimeIndex are derived to indicate time stamp. Section 3.5 briefly describes the preprocessing processes.

3.1 Solar power generation data

Hourly power generation data are collected from Yeongam solar power plant located in South Korea. The time-series data has two seasonal features – intra-year and intra-day. Fig. 2 presents the intra-year seasonality. The power generation level is very low at the beginning of a year but increases as spring arrives. During the rainy season in the months of June and July, the air in Korea is highly humid, and solar power generation generally decreases. The hourly data is aggregated every 3 h from 5 am to 8 pm, with each segment matching the weather forecast interval by KMA. A time index variable named TimeIndex is assigned accordingly, as shown in Table 1(e).

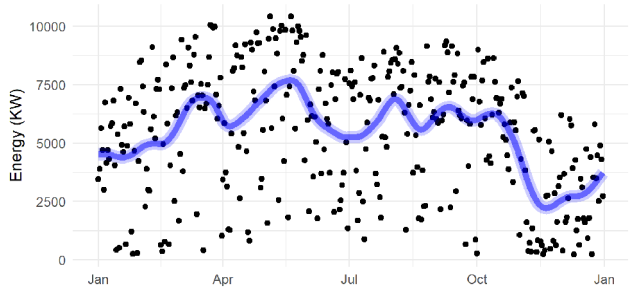

Fig. 2 *Daily solar power generation at Yeongam solar power plant from January 2015 to December 2015. Cubic smoothing spline is applied with degree of freedom of 20 [35]*

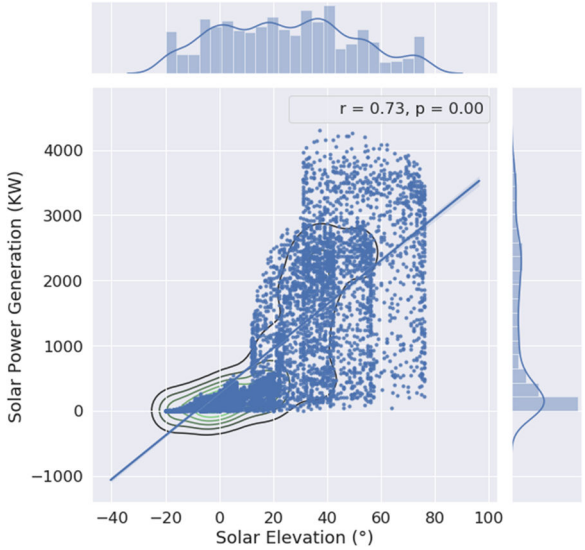

Fig. 3 *Scatter plot of solar power generation versus solar elevation*

3.2 Solar elevation data

Since higher solar altitude incurs more solar radiation, the spatial solar position is an important factor. The variable named as Elevation in Table 1(b), the vertical angular position of the sun relative to the horizon of the power plant is collected from Stellarium®.

The scatter plot for solar elevation and solar power generation is presented in Fig. 3. Two attached panels, located on the top and on the right, show the distribution of the two variables. It is noticeable that the distribution of the solar power generation is heavy-tailed. The angular solar position has a strong positive correlation with solar power generation. The sample correlation (r) is 0.73 and its p-value is less than 0.01 as annotated.

3.3 Weather forecast data

This study collects seven weather forecast variables from KMA as listed in Table 1(c). This subsection performs explorative analysis on them.

Fig. 4*a* presents the relationship between four continuous weather forecast variables and solar power generation levels. Humidity has little significance; higher RainfallProbability and WindSpeed affect the energy generation negatively, obviously because on rainy and windy days there is less sunshine; higher Temperature promotes energy generation. Fig. 4*b* presents how the three categorical weather forecast variables are related to PV power generation. The forecasts of RainfallType and SkyType are related to solar power generation in such a way that clearer sky without rain or snow incurs more solar power generation.

3.4 Weather observation data

This study collects 16 weather forecast variables from KMA as listed in Table 1(d), and they are explored in this subsection. This study seeks to exploit information content of weather observations that weather forecasts may not contain. This hypothesis is based on a few characteristics of weather observations compared to weather forecasts. First, weather agencies including KMA measure and report more number of variables in weather observation. Likewise, the weather observation data of this study have 15 variables compared to seven of weather forecasts. For example, weather observation data provide more specific and various temperature variables such as AirTemperature, GroundTemperature, 5 cm-, 10 cm-, 20 cm-, and 30 cm-GroundTemperature. Second, weather observation variables are measured in the finer units. For example, sky condition is measured as the continuous variables of SolarRadiation and SunlightTime, instead of the categorical variable of SkyType in weather forecasts. These properties of more variables in finer units, along with the higher accuracy compared to predicted values, may indicate richer information content in weather observations.

Fig. 5*a* presents the relationship between six temperature-related variables and the power generation. Though all six variables exhibit similar patterns, GroundTemperature has the highest correlation. Since 5 cm-, 10 cm-, 20 cm-, and 30 cm-GroundTemperature exhibit similar patterns and should be highly correlated with each other, this study removes all but 5 cm-GroundTemperature that has the highest correlation with the dependent variable among them. The three pressure-related variables in Fig. 5*b* exhibit common patterns, but are not much correlated to the solar power generation. Among the other variables presented in Fig. 5*c*, both of solar-related variables, SolarRadiation and SunlightTime, are highly correlated to the solar power generation. Variables of Humidity and Precipitation are negatively correlated to the solar power generation. Interestingly, the effect of dispersion in WindDirection shown in Fig. 5*c* is greater than that in Fig. 4*b*. That is, WindDirection in the forecast affects little dispersion to solar generation, but actual weather record of WindDirection seems related to the solar generation. This implies that the forecasts on the variable of WindDirection are not that accurate.

3.5 Data normalisation and temporal segmentation

Standard inputs for deep neural networks are numeric values in the bounded range [36]. Thus, categorical variables are converted into multiple binary variables, and all variables are rescaled into the range of [0, 1] by

$$\tilde{x}_i = \frac{x_i - x_{\min}}{x_{\max} - x_{\min}} \tag{1}$$

Since the LSTM network takes the input data as a time-series vector, temporal segmentation is performed for the weather observation data. One of the important design elements of an LSTM network is how many recent data points should be used as delayed inputs. As each day contains five time stamps, this study considers three alternatives of using the records of the recent 1 day (i.e. using 5 recent records), 2 days (i.e. using 10 recent records), or 3 days (i.e. using 15 recent records). Later in Section 4.2, the optimal value for hyperparameter, look_back_days, turns out to be 2, indicating that using the last 10 records of weather observation leads the best performance.

4 Prediction networks

This study builds multiple deep neural networks that find prediction models for the value of 24-hour-ahead solar power generation. That is, if the current time is 5 pm, then the model generates the predicted value of the power generation between 5 pm and 8 pm tomorrow using the currently available information. This section describes the network development processes.

After the networks are constructed, historical data are assigned to the input and output layers. The weights of the networks are initially randomly assigned. In the training process, the value of the neuron of the output layer, *generation*, is computed using the initial weights. The difference between the computed value using the

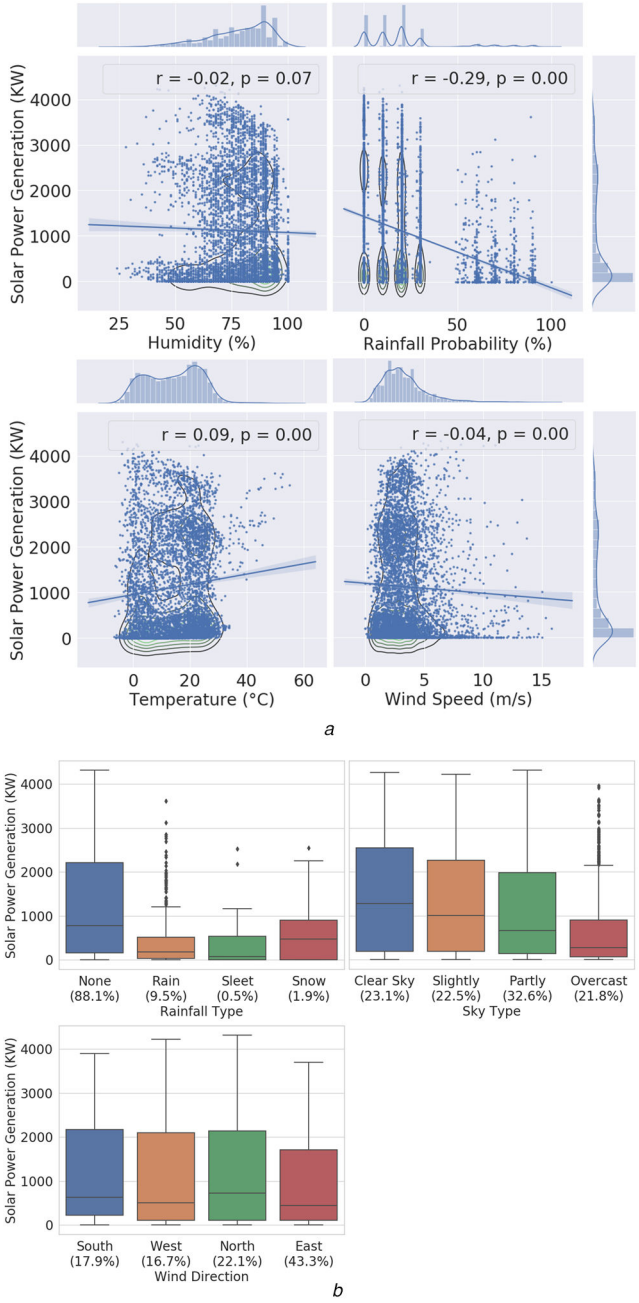

Fig. 4 *Relationship between weather forecast variables and solar power generation*

(a) Continuous variables, ***(b)*** Categorical variables

current network and the actual value provides feedback that improves the weights. The feedback is propagated back from the output layer to the input layer. The comparison and back propagation process is iteratively performed so that the initially random weights are optimised for prediction. Hyperparameter tuning processes are performed using the grid search method with the training dataset over the first 60% (21.6 months) and the validation dataset over the next 20% (7.2 months) of the entire dataset in three years (2013–2015). The rest (last 7.2 months of the year of 2015) are used as the test dataset.

A non-time-series type of network, DFN is employed to utilise weather forecast. A time-series type of network, LSTM is employed to utilise the time-series data of weather observations. Lastly, these two networks are combined to utilise both weather information. The three deep neural networks for solar power prediction are described in Table 2. The fcst-DFN builds DFN whose primary input data are weather forecast. The obs-LSTM builds a LSTM network whose primary input data are weather observation. The last network named PVHybNet uses the structure of both networks by concatenating the neurons in the last layers. Each subsection of Section 4 formulates the problem that a deep neural network aims to solve, the structure of the network, and selected hyperparameters.

4.1 fcst-DFN: DFN for weather forecast data

In utilising weather forecast information, one can match the target forecast time with the future solar power production time. That is, if the current time is t and the goal is to predict the energy generation at time $t+5$ (24 h after time t), then the weather forecasts for the target time $t+5$ is available to use at the current time t. Using the weather forecast for prediction can be formulated as an optimisation problem

$$\min_f L(y_{t+5}, \hat{y}_{t+5}) \text{ s.t. } \hat{y}_{t+5} = f(\hat{\boldsymbol{x}}_{t+5}) \tag{2}$$

where L is a loss function, $\hat{\boldsymbol{x}}$ is a vector of forecast values for weather forecast and other independent variables, y is the level of solar power generation, and $\hat{y}$ is its estimated value.

Since the input and output of the function f has same time stamp and the function f is presumably more complex than linear form, this study builds a DFN, named fcst-DFN, to identify the optimal function. Throughout this study, the metric of mean squared error is used for the loss function, which is generally used for this line of study [19].

Fig. 6 depicts the structure of fcst-DFN. The input layer has 19 features that are mainly from weather forecast variables, and features for the solar elevation and two temporal variables are also included in the input layer. Each hidden layer consists of several neurons whose values are computed by applying an activation function to the weighted sum of the neurons in the previous layer. The neurons in the output layer represent the dependent variable, *generation*.

The input data travel through the multiple hidden layers of the network, and the output of the final layer yields the prediction of solar power generation.

Table 3 lists the tested candidate values for each hyperparameter. As a hyperparameter tuning result, a network that has seven hidden layers, 20 neurons, and tanh activation function is selected. The initial weight should be assigned by the Glorot normal method and regularisation should be done with the dropout rate of 0.2. Network training should be performed with a batch size of 100, Nadam optimiser, and 256 epoch repetitions.

4.2 obs-LSTM: LSTM network for weather observation data

Weather observations for the time of actual energy generation are not available until the actual operation, but recent weather fluctuations are still relevant for predicting the level of energy generation. For example, a streak of hot hours is likely to keep solar panels hot, increasing their efficiency for the collection of solar radiation and the conversion of light energy into electricity. Motivated to utilise the temporal information, this study implements an LSTM network, named obs-LSTM, whose main input is weather observations.

Since the prediction is for solar power generation at time $t+5$ when the current time is t, the problem can be formulated as to find the best function g that solves

$$\min_g L(y_{t+5}, \hat{y}_{t+5}) \text{ s.t. } \hat{y}_{t+5} = g(\boldsymbol{x}_t, \boldsymbol{x}_{t-1}, \ldots, \boldsymbol{x}_{t-(n-1)}) \tag{3}$$

where L is a loss function, $\boldsymbol{x}$ is a vector consisting of weather observations and other independent variables, y is the level of solar power generation, $\hat{y}$ is its estimated value, and n is the number of the recent records used for prediction. Note that $n = 5$ means 1-day lookback period, $n = 10$ means 2-day lookback period, and so on.

Fig. 7 presents the structure of obs-LSTM. The input layer has 25 features that are mainly from weather observation variables, and features for the solar elevation and the temporal variables are also included. The hidden layer possesses the LSTM layers which process the time-series data. Unlike feedforward neural network including the fcst-DFN, a LSTM layer has an architecture that remembers only important information and forgets irrelevant

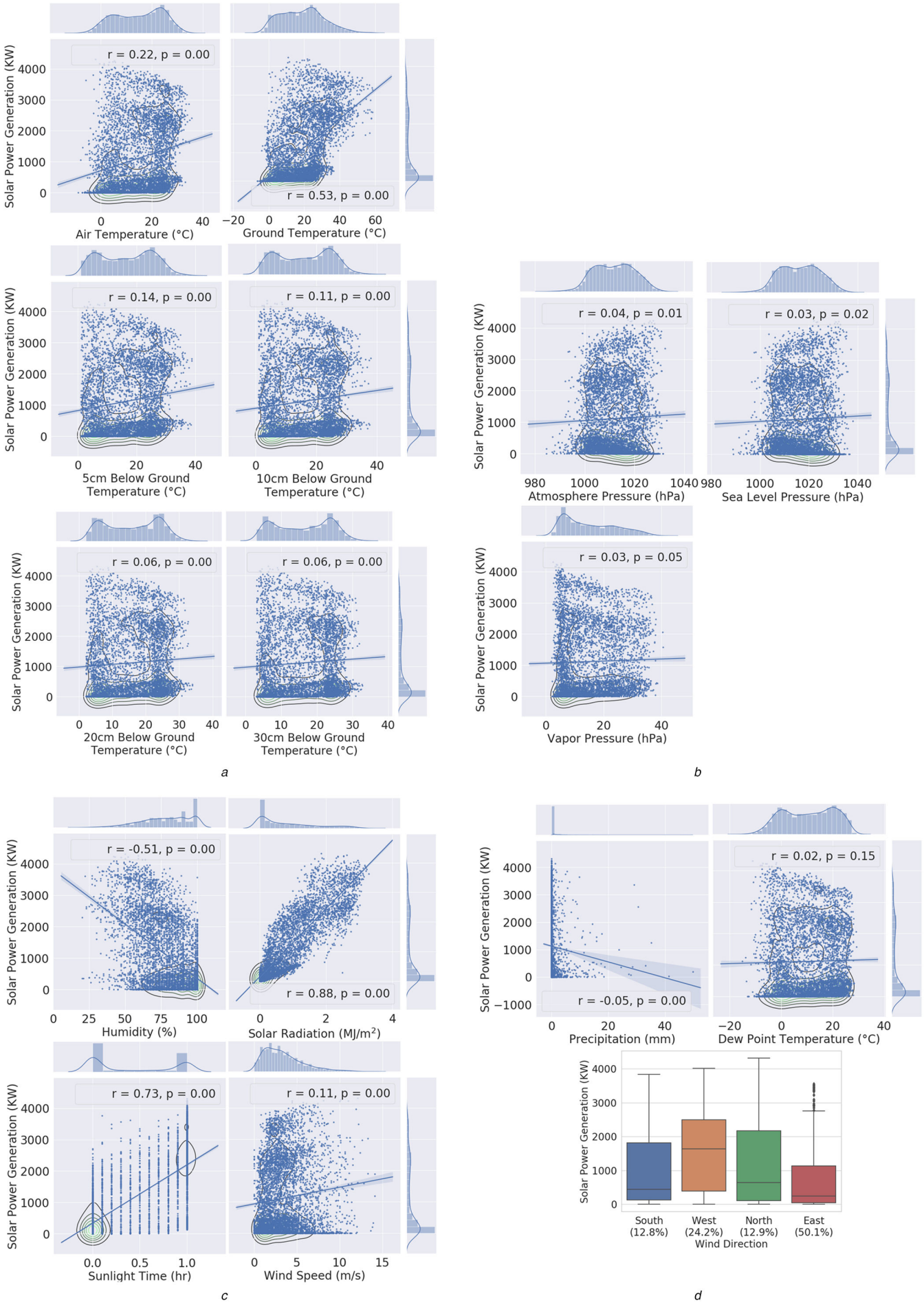

Fig. 5 *Relationship between weather observation variables and solar power generation*
(a) Temperature-related variables, ***(b)*** Pressure-related variables, ***(c)*** Other variables

Table 2 Three deep neural networks for solar power prediction

Network	Property	Description
fcst-DFN (Section 4.1)	input	weather forecast, solar elevation, temporal variables
	network type	DFN
	hypothesis	if weather forecasts are highly accurate, then a certain non-linear transformation of the forecasts can generate an accurate prediction
obs-LSTM (Section 4.2)	input	weather observation, solar elevation, temporal variables
	network type	LSTM network
	hypothesis	recent weather fluctuations contain a certain time-continuity. Thus, time-series prediction using the historical values is possible
PVHybNet (Section 4.3)	input	weather forecast, weather observation, solar elevation, temporal variables
	network type	both DFN and LSTM networks are combined
	hypothesis	since each of the above two networks has its own benefit, combining both networks can achieve both benefits. That is, this network can exploit all relevant weather information

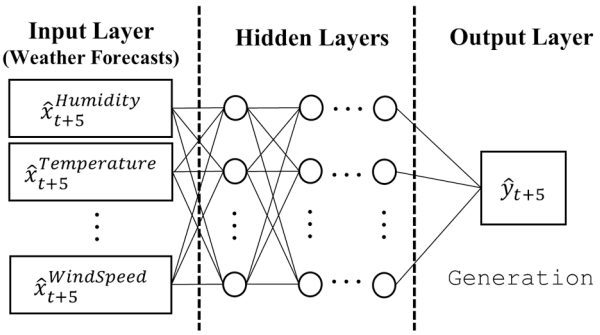

Fig. 6 *Network structure for fcst-DFN*

Table 3 Hyperparameter tuning using grid search for fcst-DFN

Hyperparameter	Candidates
number of hidden layers	1, 2, 3, 4, 5, 6, **7**, 8, 9
number of neurons in each hidden layer	10, 15, **20**
activation function	ReLU, **tanh**, hard sigmoid
dropout	**0.2**, 0.3
initialiser	**Glorot normal**, glorot uniform,
optimiser	RMSProp, Adam, **Nadam**
epochs	64, 128, **256**
batch size	**100**, 200, 500

The best values are in underlined boldface.

information. This mechanism allow LSTM layer to generate forecasted values of the input time-series data. The input data travel through individual LSTM layers, and the temporal dependency is to be understood. The output neurons from the LSTM layers are concatenated to match the dependent variable. Thus, forecast for *generation* is produced.

Table 4 lists the tested candidates for each hyperparameter. As a result, using the recent 2-day records (i.e. the recent 10 records) is the best among others. Each LSTM layer should have 20 neurons with tanh activation function with dropout rate of 0.2. The optimal recurrent dropout rate is 0.3 for regularisation. The optimiser needs to apply a batch size of 100, 256 epoch repetitions, and an optimisation algorithm of RMSProp.

4.3 PVHybNet: combining fcst-DFN and obs-LSTM

Given that both of the above neural networks are quite effective, this subsection combines them to generate more accurate predictions. The combined network, named PVHybNet, features an integrated structure that processes all relevant information including both weather forecasts and weather observations.

Formally, the network PVHybNet aims to find the best function f, g, and h that solve

$$\begin{aligned} &\min_{(f,g,h)} L(y_{t+5}, \hat{y}_{t+5}) \\ &\text{s.t.} \quad \hat{y}_{t+5} = h\big(f(\hat{\boldsymbol{x}}_{t+5}), g(\boldsymbol{x}_t, \boldsymbol{x}_{t-1}, \ldots, \boldsymbol{x}_{t-(n-1)})\big) \end{aligned} \tag{4}$$

where L is a loss function, $\hat{\boldsymbol{x}}$ is a vector of forecast values for weather forecast and other independent variables, $\boldsymbol{x}$ is a vector consisting of weather observations and other independent variables, y is the level of solar power generation, and $\hat{y}$ is its estimated value. The functions f and g process forecast values and observed values, respectively. The output of f and g are concatenated into the vector which the function h processes to generate predicted values.

Fig. 8 presents the structure of PVHybNet. The input layer has 44 features that are under consideration. The input layer handles the weather forecasts and the weather observations separately into modular networks similar to fcst-DFN and obs-LSTM, respectively. These two modular networks correspond to the functions f and g in (4) as well. The outputs from the two modular networks are then combined at the concatenation layer, and the concatenated vector finally generates the prediction value.

Table 5 lists the tested candidates for each hyperparameter and the selected values. In the modules resembling the fcst-DFN and obs-LSTM, all values of the optimal hyperparameters are identical to those in the above networks, confirming that similarly structured information is travelling as before. In the optimisation process, it turns out that more number of epochs (512 compared to 128 and 256 in the two previous networks, respectively) yields the better result.

5 Results

This section describes the performances of the proposed models and the benchmark models that are generated by popular machine learning methods.

Table 6 summarises the performance of models generated by each method. The three performance measures are employed as widely used in this line of study [19]

$$\text{RMSE} = \sqrt{\sum_{i=1}^{N} (y_i - \hat{y}_i)^2 / N} \tag{5}$$

$$\text{MAE} = \sum_{i=1}^{N} |y_i - \hat{y}_i| / N \tag{6}$$

$$R^2 = \sum_{i=1}^{N} (\hat{y}_i - \bar{y})^2 / \sum_{i=1}^{N} (y_i - \bar{y})^2 \tag{7}$$

where y_i is an actual value, $\hat{y}_i$ is a predicted value, $\bar{y}$ is the mean of the actual values, and N is the number of samples. The RMSE metric penalises large errors by using a square function. The MAE measures the average distance between predicted and actual values. The R^2 value measures the extent to which predictions are correlated with true values. Section 5.1 discusses the performances of the models generated by deep neural networks. Section 5.2 compares them against the model generated by other popular machine learning algorithms.

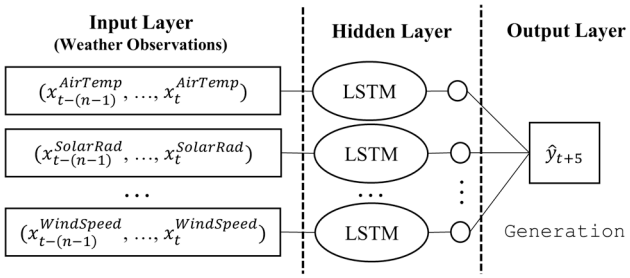

Fig. 7 *Network structure for obs-LSTM*

Table 4 Hyperparameter tuning using grid search for obs-LSTM

Hyperparameter	Candidates
look_back_days	1, **2**, 3
number of neurons in each hidden layer	5, 10, **20**
recurrent activation	ReLU, **tanh**
recurrent dropout	0.2, **0.3**
activation	ReLU, **tanh**
dropout	**0.2**, 0.3
optimiser	**RMSProp**, Adam
epochs	64, 128, **256**
batch size	**100**, 200, 500

The best values are in underlined boldface.

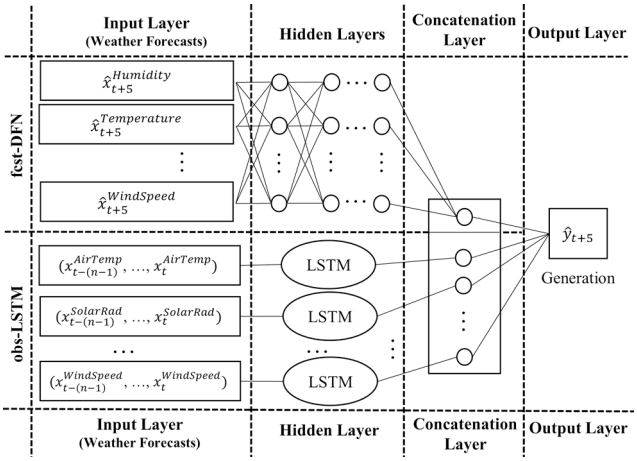

Fig. 8 *Network structure for PVHybNet*

Table 5 Hyperparameter tuning using grid search for PVHybNet

Module	Hyper-parameter	Candidates
module similar to fcst-DFN	number of neurons in each hidden layer	10, 15, **20**
	activation	ReLU, tanh, **hard sigmoid**
	dropout	0.2, **0.3**
module similar to obs-LSTM	number of neurons in each hidden layer	5, 10, **20**
	activation	ReLU, **tanh**
	dropout	**0.2**, 0.3
overall	optimiser	RMSProp, Adam, **Nadam**
	epochs	64, 128, 256, **512**
	batch size	**100**, 200, 500

The best values are in underlined boldface.

5.1 Performance of models generated by deep neural networks

In the comparison between fcst-DFN and obs-LSTM, the model by obs-LSTM outperforms the one by fcst-DFN in a wide margin in all aspects. The R^2 value for the obs-LSTM is 16.1% higher than that for fcst-DFN (Table 6). Fig. 9 provides time-series plots for two weeks of the test set (14 October 2015 to 31 October 2015). We interpret this result as follows:

- *Accuracy of weather observation*: Weather forecast is prone to prediction errors in nature. On the other hand, weather observations provide factually accurate information. For example, the box plot for actual WindDirection (Fig. 5*c*) implies that the direction of wind is related to the level of energy generation. However, the box plot for forecast values of WindDirection (Fig. 4*b*) does not reveal this relationship. This implies that the forecast for the variable WindDirection is not that accurate. The inaccuracy in forecasts may cause the poorer performance of fcst-DFN compared to obs-LSTM.
- *Rich information of weather observation*: Weather observations contain more variables compared to weather forecasts. For example, the KMA records the amount of solar radiation (SolarRadiation) and the duration of sunlight period (SunlightTime), for every hour, but neither of these variables are forecasted a priori. The obs-LSTM takes advantage of the richer information content of more variables.
- *Time-series property of weather observation*: The weather observation input contains multiple adjacent records. This may cause obs-LSTM to outperform fcst-DFN, which only accepts inputs associated with a single time-point.

The ultimate network, PVHybNet, combines the two modular networks to take their advantages. Indeed, the model generated by PVHybNet performs the best among the three. The 92.7% variance in solar power generation is explained (Table 6). In addition, the difference between actual and predicted value in Fig. 9*c* is the smallest among the three plots. We confirm that the model by PVHybNet effectively processes all relevant climate information and generates fairly accurate predictions.

5.2 Comparison with other machine learning methods

To further validate, performance is compared with several regression methods. This study considers single regression methods such as linear regression, decision tree, k-NN, and ARIMA, and ensemble regression methods such as random forest and gradient boosting [5, 9, 12, 19, 25]. The hyperparameter tuning processes are set to be identical to the ones for the three proposed models. The detail information on hyperparameter candidates and selected values is presented in Table 7.

Table 6 includes the performance of the six benchmark models. It is noticeable that performance is generally better for models with higher capacity (single regression < ensemble regression < deep neural networks). Among single regression models, ARIMA model shows the best performance in terms of RMSE and R^2 for the test set (RMSE = 547 and R^2 = 78.8). This time-series method outperforms classical machine learning methods (decision tree and k-NN) in solar power prediction. Both ensemble models yield better performance than all of the four single regression models. The gradient boosting model (RMSE = 495, MAE = 325, and R^2 = 81.5) performs better than the random forest. However, both of ARIMA and gradient boosting models perform worse than obs-LSTM and PVHybNet models significantly.

6 Conclusion

Renewable energy is expected to revolutionise human life, and data-driven predictions can support efficient and sustainable renewable energy operations. Many studies have built prediction models using weather forecasts [1–9]. Other studies have adopted time-series perspectives and applied time-series regression models [10–15]. This study pursues the benefits of both approaches

Q5 **Table 6** Performances of solar power prediction models

Regression models		Validation set			Test set		
		RMSE	MAE	R^2	RMSE	MAE	R^2
single regression models	linear regression	620	480	70.2	598	473	72.9
	decision tree	601	411	72.1	592	411	73.4
	k-NN	492	318	81.3	577	**378**	74.7
	ARIMA	514	383	80.5	**547**	400	**78.8**
ensemble regression models	random forest	514	337	79.7	524	340	79.2
	gradient boosting	467	309	83.1	**495**	**325**	**81.5**
deep neural networks	fcst-DFN	553	374	78.0	521	362	75.0
	obs-LSTM	343	255	91.0	310	232	91.1
	PVHybNet	287	200	94.1	**282**	**204**	**92.7**

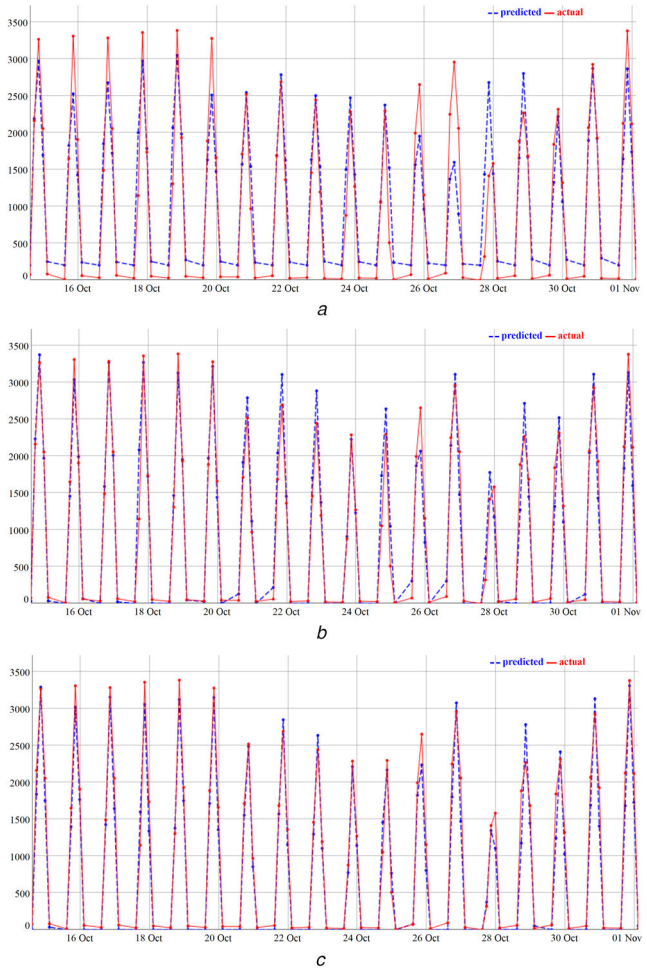

Fig. 9 *Performances of three proposed models. Test set data from 14 October 2015 to 31 October 2015 is used, where each day contains five time segments, making a total of 90 time segments*
(a) fcst-DFN, ***(b)*** obs-LSTM, ***(c)*** PVHybNet

Table 7 Hyperparameter tuning using grid search for benchmark methods

Method	Hyper-parameter	Candidates
linear reg.	none	none
decision tree	max_depth	1, 2, 3, 4, **5**, 6, 7, 8, 9, 10
k-NN	k	5, 10, **15**, 20, 40, 80
ARIMA	order	**(5, 1, 0)**
random forest	num_estimators	5, 10, 15, 20, 40, **80**
	max_depth	2, 5, **7**, 9
gradient boosting	num_estimators	5, 10, 15, 20, 40, **80**
	max_depth	2, **5**, 7, 9

The best values are in underlined boldface.

because, in our opinion, weather forecasts are the standard source of prediction power, while weather records also contain a significant information on temporal dependencies. The first network fcst-DFN, constituted by the DFN that processes forecast data, demonstrates performance comparable to other benchmark methods. The second network obs-LSTM, constituted by the LSTM network that processes the recent weather observation data, yields far better results than the benchmark methods. Finally, this study proposes PVHybNet that combines the two deep neural networks. This ultimate network yields an R^2 value of 92.7% in the test set, demonstrating a significant improvement over the performances of the two individual networks and the other benchmark methods.

To improve the performance further, it is conceivable that other power-plant operation data in addition to the amount of production can be utilised. More accurate and rich weather data will obviously improve the model's performance as well. For example, more granular weather time-series data will enable real-time predictions to support more efficient production planning and monitoring. As renewable energy becomes more important, weather agencies are expected to expand the availability of weather variables that are closely related to operations.

Due to the high relevance to climate conditions, prediction of solar power generation is naturally a location-specific. However, the approach and modelling methodology proposed in this study are not limited to specific geography. Future studies can adopt our approach to solar power plants around the world to obtain insights and knowledge of their future PV power production.

7 References

[1] Sharma, N., Sharma, P., Irwin, D., *et al.*: 'Predicting solar generation from weather forecasts using machine learning'. Proc. of the Int. Conf. on SmartGridComm, Brussels, Belgium, October 2011, pp. 528–533

[2] Chaouachi, A., Kamel, R.M., Ichikawa, R., *et al.*: 'Neural network ensemble-based solar power generation short-term forecasting', *World. Acad. Sci. Eng. Technol.*, 2009, **3**, (6), pp. 1258–1263

[3] Sharma, N., Gummeson, J., Irwin, D., *et al.*: 'Cloudy computing: leveraging weather forecasts in energy harvesting sensor systems'. Proc. of the Int. Conf. on SECON, Boston, Massachusetts, U.S.A., June 2010, pp. 1–9

[4] Li, Y., Su, Y., Shu, L.: 'An Armax model for forecasting the power output of a grid connected photovoltaic system', *Renew. Energy*, 2014, **66**, pp. 78–89

[5] Persson, C., Bacher, P., Shiga, T., *et al.*: 'Multi-site solar power forecasting using gradient boosted regression trees', *Sol. Energy*, 2017, **150**, pp. 423–436

[6] Leva, S., Dolara, A., Grimaccia, F., *et al.*: 'Analysis and validation of 24 H ahead neural network forecasting of photovoltaic output power', *Math. Comput. Simul.*, 2017, **131**, pp. 88–100

[7] Amrouche, B., Le Pivert, X.: 'Artificial neural network based daily local forecasting for global solar radiation', *Appl. Energy*, 2014, **130**, pp. 333–341

[8] Gensler, A., Henze, J., Sick, B., *et al.*: 'Deep learning for solar power forecasting—an approach using autoencoder and LSTM neural networks'. Proc. of the Int. Conf. on SMC, Budapest, October 2016, pp. 2858–2865

[9] Andrade, J.R., Bessa, R.J.: 'Improving renewable energy forecasting with a grid of numerical weather predictions', *IEEE Trans. Sustain. Energy*, 2017, **8**, (4), pp. 1571–1580

[10] Hossain, M.R., Oo, A.M.T., Ali, A.S.: 'Hybrid prediction method of solar power using different computational intelligence algorithms'. Proc. of the 22nd Int. Conf. on AUPEC, Bali, Indonesia, September 2012, pp. 1–6

[11] Bacher, P., Madsen, H., Nielsen, H.A.: 'Online short-term solar power forecasting', *Sol. Energy*, 2009, **83**, (10), pp. 1772–1783

[12] Zamo, M., Mestre, O., Arbogast, P., *et al.*: 'A benchmark of statistical regression methods for short-term forecasting of photovoltaic electricity production, part I: deterministic forecast of hourly production', *Sol. Energy*, 2014, **105**, pp. 792–803

[13] Alzahrani, A., Shamsi, P., Dagli, C., *et al.*: 'Solar irradiance forecasting using deep neural networks', *Procedia Comput. Sci.*, 2017, **114**, pp. 304–313
[14] Li, L.-L., Cheng, P., Lin, H.-C., *et al.*: 'Short-term output power forecasting of photovoltaic systems based on the deep belief net', *Adv. Mech. Eng.*, 2017, **9**, (9)
Q1 [15] Kim, J.-G., Kim, D.-H., Yoo, W.-S., *et al.*: 'Daily prediction of solar power generation based on weather forecast information in Korea', *IET Renew. Power Gener.*, 2017, **11**, (10), pp. 1268–1273
[16] Detyniecki, M., Marsala, C., Krishnan, A., *et al.*: 'Weather-based solar energy prediction'. Proc. of the Int. Conf. FUZZ-IEEE, Brisbane, Australia, June 2012, pp. 1–7
[17] Abedinia, O., Raisz, D., Amjady, N.: 'Effective prediction model for Hungarian small-scale solar power output', *IET Renew. Power Gener.*, 2017, **11**, (13), pp. 1648–1658
[18] Antonanzas, J., Osorio, N., Escobar, R., *et al.*: 'Review of photovoltaic power forecasting', *Sol. Energy*, 2016, **136**, pp. 78–111
[19] Voyant, C., Notton, G., Kalogirou, S., *et al.*: 'Machine learning methods for solar radiation forecasting: a review', *Renew. Energy*, 2017, **105**, pp. 569–582
[20] Barbieri, F., Rajakaruna, S., Ghosh, A.: 'Very short-term photovoltaic power forecasting with cloud modeling: a review', *Renew. Sust. Energy Rev.*, 2017, **75**, pp. 242–263
[21] Inman, R.H., Pedro, H.T., Coimbra, C.F.: 'Solar forecasting methods for renewable energy integration', *Prog. Energy Combust. Sci.*, 2013, **39**, (6), pp. 535–576
[22] Gueymard, C.A., Ruiz-Arias, J.A.: 'Extensive worldwide validation and climate sensitivity analysis of direct irradiance predictions from 1-min global irradiance', *Sol. Energy*, 2016, **128**, pp. 1–30
[23] Kim, S., Jung, J., Sim, M.: 'A two-step approach to solar power generation prediction based on weather data using machine learning', *Sustainability*, 2019, **11**, (5), p. 1501
[24] Abuella, M., Chowdhury, B.: 'Improving combined solar power forecasts using estimated ramp rates: data-driven post-processing approach', *IET Renew. Power Gener.*, 2018, **12**, (10), pp. 1127–1135
[25] Pedro, H.T., Coimbra, C.F.: 'Assessment of forecasting techniques for solar power production with no exogenous inputs', *Sol. Energy*, 2012, **86**, (7), pp. 2017–2028
[26] Bishop, C.M.: '*Pattern recognition and machine learning*' (Springer Press, 2006)
Q2 [27] Shao, H., Soong, B.-H.: 'Traffic flow prediction with long short-term memory networks (Lstms)'. 2016 IEEE Region 10 Conf. (TENCON), pp. 2986–2989
Q3 [28] Zhu, Y., Dai, R., Liu, G., *et al.*: 'Power market price forecasting via deep learning'. IECON 2018-44th Annual Conf. of the IEEE Industrial Electronics Society, pp. 4935–4939
[29] Cortez, B., Carrera, B., Kim, Y., *et al.*: 'An architecture for emergency event prediction using LSTM recurrent neural networks', *Expert Syst. Appl.*, 2018, **97**, pp. 315–324
[30] Park, D., Kim, S., An, Y., *et al.*: 'Lired: A light-weight real-time fault detection system for edge computing using LSTM recurrent neural networks', *Sensors*, 2018, **18**, (7), p. 2110
[31] Abdel-Nasser, M., Mahmoud, K.: 'Accurate photovoltaic power forecasting models using deep LSTM-RNN', *Neural Comput. Appl.*, 2017, pp. 1–14
Q4 [32] 'Korea open data portal', Available at https://www.data.go.kr/, accessed May 2018
[33] 'Stellarium', Available at https://stellarium.org/, accessed June 2018
[34] 'Korea meteorological administration', Available at https://data.kma.go.kr/cmmn/main.do, accessed June 2018
[35] Hastie, T.J.: '*Generalized additive models, statistical models in S*' (Routledge, 2017)
[36] Abadi, M., Barham, P., Chen, J., *et al.*: 'Tensorflow: a system for large-scale machine learning'. Proc. of the Int. Conf. OSDI, Savannah, Georgia, U.S.A., November 2016, pp. 265–283

Author Queries

Q Please make sure the supplied images are correct for both online (colour) and print (black and white). If changes are required please supply corrected source files along with any other corrections needed for the paper.
Q1 Please provide page range in Ref. [14].
Q2 Please provide the location of the publisher (country) in Refs. [26, 35].
Q3 Please provide year of publication and place of conference in Refs. [27, 28].
Q4 Please provide volume number in Ref. [31].
Q5 Please provide the significance of bold in Table 6.